Title

Type II Anion Relay Chemistry: Conformational Constraints To Achieve Effective [1,5]-Vinyl Brook Rearrangements

Journal

Journal of the American Chemical Society, 139(25)

ISSN

0002-7863

Authors

Liu, Qi
Chen, Yu
Zhang, Xiao
et al.

Publication Date

2017-06-28

DOI

10.1021/jacs.7b04149

Peer reviewed

HHS Public Access

Author manuscript

J Am Chem Soc. Author manuscript; available in PMC 2018 June 28.

Published in final edited form as:

J Am Chem Soc. 2017 June 28; 139(25): 8710–8717. doi:10.1021/jacs.7b04149.

Type II Anion Relay Chemistry: Conformational Constraints To Achieve Effective [1,5]-Vinyl Brook Rearrangements

Qi Liu[†], **Yu Chen**[‡], **Xiao Zhang**[‡], **K. N. Houk**[§], **Yong Liang**[*,‡], and **Amos B. Smith III**[*,†]

[†]Department of Chemistry, University of Pennsylvania, Philadelphia, Pennsylvania 19104, United States

[‡]State Key Laboratory of Coordination Chemistry, School of Chemistry and Chemical Engineering, Nanjing University, Nanjing 210023, China

[§]Department of Chemistry and Biochemistry, University of California, Los Angeles, California 90095, United States

Abstract

The design, synthesis, and evaluation of bifunctional linchpins, conformationally anchored on six-membered rings to achieve efficient [1,5]-Brook rearrangements involving vinyl silanes have been achieved. The restrained linchpins were subsequently exploited in type II anion relay chemistry (ARC) to permit both alkylations and Pd-mediated cross-coupling reactions (CCR) of sp^2 stabilized carbanions. DFT calculations were then employed to understand the mechanism and reactivity trends of [1,4]- and [1,5]-vinyl Brook rearrangements to provide insight on the role of the required copper reagent and the substrate geometry.

Graphical abstract

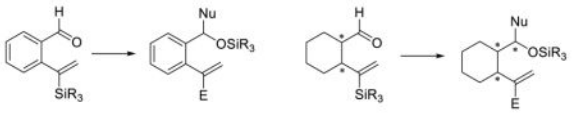

[*]Corresponding Authors: yongliang@nju.edu.cn. smithab@sas.upenn.edu.

ORCID

K. N. Houk: 0000-0002-8387-5261

Yong Liang: 0000-0001-5026-6710

Amos B. Smith III: 0000-0002-1712-8567

Notes

The authors declare no competing financial interest.

Supporting Information

The Supporting Information is available free of charge on the ACS Publications website at DOI: 10.1021/jacs.7b04149.

Experimental procedures and computational details (PDF)

NMR spectra for obtained compounds (PDF)

X-ray data for compound 26 (CIF)

X-ray data for compound 27 (CIF)

INTRODUCTION

In 2005, we defined a new platform for the construction of molecular complexity termed anion relay chemistry (ARC; Scheme 1).[1] Critical to the success of this tactic is the ability to migrate charge in a controlled manner from an oxygen to a carbon atom, bearing an anion stabilizing group (ASG), during a reversible Brook rearrangement.[2]

The dithiane group, introduced by Corey and Seebach[3] for umpolung reactions and subsequently exploited by the Schaumann[4] and Tietze[5] groups for what we now view as early versions of the ARC tactic, has proven to be an excellent ASG for both type I and type II ARC transformations involving [1,4]-Brook rearrangements.[6] Indeed, by employing a series of diverse dithiane ARC linchpins, a number of architecturally complex targets have been achieved, as demonstrated in synthetic ventures toward spirastrellolide E,[7] (−)-secu'amamine A,[8] rhizopodin,[9] enigmazole A,[10] and most recently mandelalide A.[11]

Following the success of the ARC tactic exploiting the dithiane as an sp^3 carbon ASG, several linchpins were subsequently designed, synthesized, and validated to exploit sp^2-hybridized carbons in [1,4]-Brook rearrangements. Anions derived from furans,[12] arenes, and olefins were employed.[13] During this study, the stability of the sp^2 carbanion derived from arenes and olefins during the reversible O to C(sp^2) Brook rearrangement, not surprisingly, proved less favorable compared to the C(sp^3) dithiane stabilized carbanions. To augment the sp^2 based ARC tactic, we introduced a stabilization factor, via the formation of an organocuprate.[13,14]

The latter permitted the successful validation of vinyl silanes bearing β or γ electrophilic carbonyl sites for type II ARC transformations based on [1,4]-Brook rearrangements.[13] During these earlier studies, we recognized however that the Brook rearrangement was quite sensitive to the specific location of the silyl group on the double bond. The conditions that proved effective for linchpin **10** (1.2 equiv of *n*-BuLi and CuI; Scheme 2) did not permit facile [1,4]-silyl migration with linchpin **12**. In this case, 2 equiv of both *n*-BuLi and CuI were required to complete the 1,4-silyl C(sp^2) to O migration over the course of a 2 h period at room temperature (Scheme 2).[13] At the time, it was not clear why a second equivalent of *n*-BuLi and CuI significantly improved the [1,4]-vinyl Brook rearrangement of **12.**

Recognizing that [1,5]-Brook rearrangements with vinyl linchpins, and in particular linchpins with terminal olefins held considerable promise for the construction of molecular complexity, we began to investigate an ARC tactic based on [1,5]-silyl C(sp^2) to O migrations (Figure 1).[15] We reasoned that anchoring the requisite ARC functionality on a phenyl or cyclohexyl ring in a 1,2 fashion would limit bond rotation and thereby potentially enhance the [1,5]-Brook rearrangement.

RESULTS AND DISCUSSION

To initiate this study, we prepared phenyl linchpin **14** via Negishi cross coupling of (1-trimethylsilyl)-vinyl zinc with 2-bromo-benzaldehyde (see Supporting Information). Our initial conditions for the [1,5]-Brook rearrangement were derived from our previous work involving [1,4]-silyl C(sp^2) to O migration,[13] as well as from earlier observations of the

Takeda[16] and Song groups.[17] Specifically, after addition of 2 equiv of *n*-BuLi to aldehyde **14**, the resulting lithium alkoxide was added into a suspension of CuBr·DMS in HMPA and THF (1:1) via cannula to trigger the Brook rearrangement, presumably permitting the formation of a vinyl-cuprate. Importantly, we subsequently discovered that in place of adding 2 equiv of the required nucleophile, an additive (i.e., 1 equiv of a *tert*-butoxide salt) could be employed to achieve similar results, thus eliminating the need for 2 equiv of the potentially valuable nucleophile. The vinyl-cuprate was then subjected to alkylation with a variety of electrophiles to furnish three-component adducts in modest to good yields (Table 1).

The organocuprate generated from the [1,5]-Brook rearrangement was next evaluated for cross coupling with various electrophilic partners, employing $Pd(PPh_3)_4$ as the catalyst (Table 2). Both electron-deficient and -rich aryl iodides proved viable substrates under the ARC/CCR protocol. Vinyl bromide could also be employed as the cross-coupling partner to provide diene **16e**. In addition to *n*-BuLi, methyl, phenyl, 2-methyl vinyl, 2-furanyl, and 2-methyl-1,3-dithianyl lithiums were examined as the initiating nucleophile for the ARC process; all worked, leading to the desired three-component adducts **16f**–**16j**.

Encouraged by the viability of the ARC alkylation and cross coupling protocols exploiting a [1,5]-Brook rearrangement with phenyl linchpin **14**, we turned to evaluate cyclohexyl-based linchpins, constructed via conjugate addition[18,19] of the vinyl-cuprate derived from **17**[20] to aldehyde **18** (Scheme 3); a 1:1 mixture of *cis*- and *trans*-linchpins (**19** and **20**), separable via flash chromatography with the stereochemistry assigned by NMR, and subsequent chemical conversion (vide infra) resulted in a combined yield of 63%. Importantly, *cis*-linchpin **19** could be readily converted to the *trans*-congener (**20**) by treatment with DBU in MeOH.

With both cyclohexyl-linchpins (**19** and **20**) in hand, we first conducted an optimization study with *cis*-cyclohexyl linchpin **19** exploiting the conditions outlined in Table 3. Compared to the phenyl linchpin (**14**), an increase in reaction temperature was required to effectively trigger the [1,5]-Brook rearrangement. Again, *t*-BuOK could be employed to promote Brook rearrangement, thus saving 1 equiv of the nucleophile, although a longer reaction time was required to complete the Brook process. In the case of the TMS linchpin, the longer reaction time unfortunately resulted in several side reactions (i.e., loss of TMS group and/or decomposition of the vinyl-cuprate). To shorten the required reaction time and thus side product formation, we increased the solvent polarity to further promote the Brook rearrangement efficiency (entry 7).

Continuing with the envisioned vinyl-cuprate intermediate derived via the [1,5]-Brook rearrangement, we introduced an electrophile to complete the tricomponent ARC tactic. As with phenyl linchpin **14**, the vinyl-cuprate was evaluated for both alkylation (Table 4) and cross coupling (Table 5); both reactions proceeded, leading to the three-component adducts in modest to good yield.

Notably, nucleophilic additions to *cis*-linchpin **19** proved highly diastereoselective (>20:1), yielding the Felkin–Anh product,[21] which was confirmed in the case of three-component adduct **25h** by X-ray analysis of the derived 4-nitrobenzoic ester (**26**) (Figure 2).

We next extended the [1,5] ARC tactic to *trans*-linchpin **20**. High Felkin–Anh selectivity upon addition of the nucleophile to the aldehyde was achieved. The stereochemistry of the isolated product was again confirmed by X-ray analysis of the *p*-nitrobenzoic ester derivative **27** (Figure 2).

The [1,5]-Brook rearrangement of *trans*-linchpin **20** however proved more challenging than the *cis*-linchpin. In particular, difficulties were encountered in retaining the TMS silyl group during the [1,5]-Brook protocol. As a result, multiple alkylation byproducts were observed due to competing O-alkylation when an electrophile was introduced. To resolve this issue, we turned to the more robust TBS counterpart **31**, which was prepared in similar fashion as the TMS linchpin (Scheme 4). As expected, loss of the silyl group was no longer observed, but a higher reaction temperature was required to trigger Brook rearrangement, presumably due to the increased steric hindrance of the TBS group. As mentioned earlier during the optimization of *cis*-linchpin, longer reaction times resulted in multiple side reactions. In this case, decomposition of a significant amount of the vinyl-cuprate occurred. To decrease the reaction time, we employed a 5 min pulse of microwave irradiation (Biotage: high setting) at 100 °C. The derived vinyl-cuprate was then employed for three-component unions, as demonstrated by alkylation with benzyl bromide and CCR with 4-iodobenzonitrile (Scheme 4).

To understand the mechanism and reactivity trends of the [1,4]- and [1,5]-vinyl Brook rearrangements, we conducted computational studies using DFT (M06 with solvation) calculations,[22,23] in which MeLi was used as a computational model for the experimentally employed *n*-BuLi. First, three [1,4]-vinyl Brook rearrangements were compared to reveal the effect on the energetics of the position of the C═C double bond and the copper reagent employed. The results are summarized in Scheme 5, with the key structures illustrated in Figure 3.

For the [1,4]-Brook rearrangement of substrate **A** having an internal C═C double bond (Scheme 5a), coordination of the CuI to both the C═C bond and oxygen atom of **A** generates an intermediate **Ac**; this step is exergonic by 28.5 kcal/mol in THF. Subsequently, the oxygen atom attacks the trimethylsilyl group via transition state **TSA** (Figure 3), in which the forming O–Si bond distance is 1.85 Å and the breaking C–Si bond is 2.37 Å, while the C–Cu distance is decreased to 1.96 Å. The free energy barrier for this process is 16.0 kcal/mol (from **Ac** to **TSA**). Importantly, the resultant [1,4]-Brook rearrangement product **Ap** is more stable than **Ac** by 6.3 kcal/mol.

As reported above, our experimental results demonstrate that the [1,4]-Brook rearrangement is sensitive to the position of C═C double bond (Scheme 2). The computed reaction pathway of the [1,4]-Brook rearrangement of **B** having a terminal C═C double bond with 1 equiv of CuI is illustrated in Scheme 5b. In this case, the formation of intermediate **Bc** via coordination of CuI to both the C═C bond and the oxygen atom of **B** is exergonic by 35.5 kcal/mol, which is 7 kcal/mol more favorable than that of **Ac** (−35.5 versus −28.5 kcal/mol). Subsequent [1,4]-Brook free energy of 29.8 kcal/mol. This barrier is 13.8 kcal/mol higher than that for **Ac** with an internal C═C double bond (29.8 versus 16.0 kcal/mol). As shown in Figure 3, the coordination of the internal C═C double bond forms a strained C–Cu–O–C

four membered ring in **Ac**, with C–Cu and O–Cu distances of 2.10 and 2.22 Å. However, in the Brook rearrangement transition state **TSA**, the corresponding distances are significantly increased to 2.75 and 2.70 Å, respectively. This indicates that there is remarkable strain-release in transition state **TSA**, leading to a low barrier.[24] However, when the position of the C═C double bond is changed from internal to terminal, the strained C–Cu–O–C four membered ring in **Ac** evolves to an unstrained C–Cu–O–C–C–C six membered ring in **Bc**. As a result, there is no strain-release in transition state **TSB**, making the barrier much higher, and in the product (**Bp)**, which is even 0.2 kcal/mol less stable than **Bc** (−35.3 versus −35.5 kcal/mol). This result explains why the [1,4]-Brook rearrangement of **B** having a terminal C═C double bond does not occur using 1 equiv of CuI.

To achieve efficiency with the [1,4]-Brook rearrangement of **B**, experiments demonstrate that 2 equiv of a Cu(I) salt and a second equivalent of lithium reagent are required (Scheme 2). However, it was not clear what copper reagent is involved. Our calculations reveal that the most favorable reaction between 1 equiv of MeLi with 2 equiv of CuX (X = I or Br) is to form MeCu (eq 1),

$$\begin{array}{lcll} \mathrm{MeLi} & + & 2\mathrm{CuX} & \rightarrow \quad \mathrm{MeCu{+}Li^{+}{+}CuX_2^{-}} \\ & & \mathrm{X{=}I} & \quad \Delta G{=}{-}54.6\,\mathrm{kcal/mol} \\ & & \mathrm{X{=}Br} & \quad \Delta G{=}{-}58.0\,\mathrm{kcal/mol} \end{array} \quad (1)$$

which is exergonic by more than 50 kcal/mol in THF. This suggests that under these reaction conditions, MeCu instead of CuX will trigger Brook rearrangement.

In Scheme 5c, we outline the computed reaction pathway of [1,4]-Brook rearrangement of **B** with 1 equiv of MeCu. Here the MeCu is also coordinated by both the C═C bond and the oxygen atom of **B** to form intermediate **Cc**. However, this process is much less exergonic than that using CuI (−20.4 versus −35.5 kcal/mol). The subsequent [1,4]-Brook rearrangement via transition state **TSC** thus requires an activation free energy of 25.8 kcal/mol. This barrier is 4 kcal/mol lower than that using CuI (25.8 versus 29.8 kcal/mol). According to the frontier molecular orbital (FMO) analysis, the LUMO energies of CuI and MeCu are −15.3 and 1.3 kcal/mol, respectively. This indicates that CuI is a much better electron acceptor than MeCu, leading to a much stronger coordination or bonding interaction. As shown in Figure 3, the geometries of intermediates **Bc** and **Cc**, and transition states **TSB** and **TSC** are very similar. In the Brook rearrangement transition state **TSB** or **TSC**, one C–Cu bond (**TSB**, 1.96 Å; **TSC**, 1.97 Å) is forming, and one O···Cu and the other C···Cu coordinations (shown as green lines in the right structures of Figure 3) disappear. When MeCu is employed instead of CuI, two weaker O···Cu and C···Cu interactions are needed to be overcome in the transition state, although one weaker C–Cu bond is forming. Overall, this decreases the barrier for the Brook rearrangement. Therefore, the alkyl cuprate is more active than the Cu(I) salt to trigger Brook rearrangement, in agreement with the experimental results.

Four [1,5]-vinyl Brook rearrangements were next compared to reveal the role of the conformational constraints of substrates. The results are summarized in Scheme 6, with the key structures illustrated in Figure 4.

For the MeCu mediated [1,5]-Brook rearrangement of substrate **D** having a terminal C═C double bond (Scheme 6a), the reaction free energy for the coordination step is −20.1 kcal/mol, which is very close to that of [1,4]-Brook rearrangement substrate **C** (−20.4 kcal/mol, Scheme 5c). However, the barrier for the [1,5]-Brook rearrangement is 3.7 kcal/mol higher than that for the [1,4] reaction (29.5 versus 25.8 kcal/mol). As shown in Figures 3 and 4, the forming and breaking bond distances in transition states **TSC** and **TSD** are almost identical; the main difference is the conformational change of the tether. In intermediate **Dc**, the dihedral angle along the $(CH_2)_2$ tether is −73.2 °, but this angle becomes −57.9° in transition state **TSD**. This means a 15.3° conformational change, requiring additional energy as compared to [1,4]-Brook rearrangement from **Cc** to **TSC**, in which the tether is CH_2 without the dihedral angle change. This explains why efficient [1,5]-Brook rearrangements are more challenging.

In Scheme 6b–d, we illustrate the computed reaction pathways of the three experimentally studied [1,5]-vinyl Brook rearrangements involving phenyl, *cis*-cyclohexyl, and *trans*-cyclohexyl linchpins. The activation free energies for these rearrangements are 23.3 (from **Ec** to **TSE**), 25.6 (from **Fc** to **TSF**), and 29.7 (from **Gc** to **TSG**) kcal/mol, respectively. This reactivity trend is in accordance with the increase in reaction temperature for Brook rearrangement observed experimentally. More importantly, the calculations demonstrate that there is a good correlation between the conformational change of the tether and the barrier for the [1,5]-Brook rearrangement. As illustrated in Figure 4, when the tether is switched from phenyl, to *cis*-cyclohexyl, and to *trans*-cyclohexyl, the corresponding conformational change is increased from 4.8° (from −1.4° to −6.2°), to 6.1° (from −41.4° to −47.5°), and to 13.5° (from 39.8° to 53.3°). Consequently, the barrier is increased from 23.3 to 25.6 and 29.7 kcal/mol (Scheme 6b–d). These results indicate that using the tether with conformational constraints can efficiently lower the [1,5]-Brook rearrangement barrier.

CONCLUSIONS

In summary, we have achieved extension of the ARC tactic exploiting more challenging [1,5]-Brook rearrangements with a series of conformationally anchored bifunctional vinyl linchpins. Phenyl, *cis*-cyclohexyl, and *trans*-cyclohexyl linchpins were systematically evaluated via both experimental and computational approaches. Of importance, we demonstrated that introduction of an additional amount of organolithium or *t*-BuOK as additive lowers the energy barrier to facilitate the requisite Brook rearrangement. As such, this ARC protocol now holds considerable synthetic promise for the rapid elaboration of advanced intermediates for complex molecule synthesis.

Supplementary Material

Refer to Web version on PubMed Central for supplementary material.

Acknowledgments

Financial support was provided by the National Institutes of Health (National Cancer Institute) through Grant No. CA-19033 and the National Science Foundation (CHE-1361104). Y.L. thanks the National Thousand Young Talents Program and Jiangsu Specially-Appointed Professor Plan in China for financial support. We also thank China Scholarship Council for a scholarship for Q.L. We thank Drs. George Furst and Jun Gu and Dr. Rakesh Kohli at the University of Pennsylvania for help in obtaining the NMR and high-resolution mass spectral data, respectively, and Dr. Patrick J. Carroll for X- ray crystallographic data.

References

1. Smith AB, Xian M. J Am Chem Soc. 2006; 128:66. [PubMed: 16390124]
2. Brook AG. Acc Chem Res. 1974; 7:77.
3. Seebach D, Corey EJ. J Org Chem. 1975; 40:231.
4. Fischer MR, Kirschning A, Michel T, Schaumann E. Angew Chem, Int Ed Engl. 1994; 33:217.
5. Tietze LF, Geissler H, Gewert JA, Jakobi U. Synlett. 1994; 1994:511.
6. For reviews on anion relay chemistry, see: Smith AB III, Adams CM. Acc Chem Res. 2004; 37:365. [PubMed: 15196046] Smith AB III, Wuest WM. Chem Commun. 2008:5883.
7. Sokolsky A, Wang X, Smith AB. Tetrahedron Lett. 2015; 56:3160. [PubMed: 26097261]
8. Han H, Smith AB. Org Lett. 2015; 17:4232. [PubMed: 26291547]
9. Melillo B, Chen MZ, Forestieri R, Smith AB. Org Lett. 2015; 17:6242. [PubMed: 26641664]
10. Ai Y, Kozytska MV, Zou Y, Khartulyari AS, Smith AB. J Am Chem Soc. 2015; 137:15426. [PubMed: 26632969]
11. Nguyen MH, Imanishi M, Kurogi T, Smith AB. J Am Chem Soc. 2016; 138:3675. [PubMed: 26954306]
12. Devarie-Baez NO, Kim WS, Smith AB, Xian M. Org Lett. 2009; 11:1861. [PubMed: 19301924]
13. Smith AB, Kim WS, Tong R. Org Lett. 2010; 12:588. [PubMed: 20028107]
14. Taguchi H, Takami K, Tsubouchi A, Takeda T. Tetrahedron Lett. 2004; 45:429.
15. For previous success of a coupling reaction exploiting [1,5]-Brook rearrangement, see: Smith AB, Xian M, Kim WS, Kim DS. J Am Chem Soc. 2006; 128:12368. [PubMed: 16984158] Gao L, Lu J, Song Z, Lin X, Xu Y, Yin Z. Chem Commun. 2013; 49:8961.
16. Tsubouchi A, Itoh M, Onishi K, Takeda T. Synthesis. 2004; 2004:1504.
17. Yan L, Sun X, Li H, Song Z, Liu Z. Org Lett. 2013; 15:1104. [PubMed: 23410199]
18. Corey EJ, Boaz NW. Tetrahedron Lett. 1985; 26:6015.
19. Zou Y, Melvin JE, Gonzales SS, Spafford MJ, Smith AB. J Am Chem Soc. 2015; 137:7095. [PubMed: 26029849]
20. Boeckman RKJ, Blum DM, Ganem B, Halvey N. Org Synth. 1978; 58:152.
21. Anh NT, Eisenstein O. Tetrahedron Lett. 1976; 17:155.
22. Frisch, MJ., Trucks, GW., Schlegel, HB., Scuseria, GE., Robb, MA., Cheeseman, JR., Scalmani, G., Barone, V., Mennucci, B., Petersson, GA., Nakatsuji, H., Caricato, M., Li, X., Hratchian, HP., Izmaylov, AF., Bloino, J., Zheng, G., Sonnenberg, JL., Hada, M., Ehara, M., Toyota, K., Fukuda, R., Hasegawa, J., Ishida, M., Nakajima, T., Honda, Y., Kitao, O., Nakai, H., Vreven, T., Montgomery, JA., Jr, Peralta, JE., Ogliaro, F., Bearpark, M., Heyd, JJ., Brothers, E., Kudin, KN., Staroverov, VN., Kobayashi, R., Normand, J., Raghavachari, K., Rendell, A., Burant, JC., Iyengar, SS., Tomasi, J., Cossi, M., Rega, N., Millam, JM., Klene, M., Knox, JE., Cross, JB., Bakken, V., Adamo, C., Jaramillo, J., Gomperts, R., Stratmann, RE., Yazyev, O., Austin, AJ., Cammi, R., Pomelli, C., Ochterski, JW., Martin, RL., Morokuma, K., Zakrzewski, VG., Voth, GA., Salvador, P., Dannenberg, JJ., Dapprich, S., Daniels, AD., Farkas, O., Foresman, JB., Ortiz, JV., Cioslowski, J., Fox, DJ. Gaussian 09, revision D.01. Gaussian, Inc; Wallingford, CT: 2009.
23. Geometry optimizations and frequency calculations were performed at the M06/6-31G(d)[SDD, for Cu, Br, and I] level. Single-point energy calculations in THF using the CPCM model were performed at the M06/6-311+G(d,p)[SDD, for Cu, Br, and I] level. For details, see the SI.

24. (a) Hong X, Liang Y, Griffith AK, Lambert TH, Houk KN. Chem Sci. 2014; 5:471.(b) Zou L, Paton RS, Eschenmoser A, Newhouse TR, Baran PS, Houk KN. J Org Chem. 2013; 78:4037. [PubMed: 23461537]

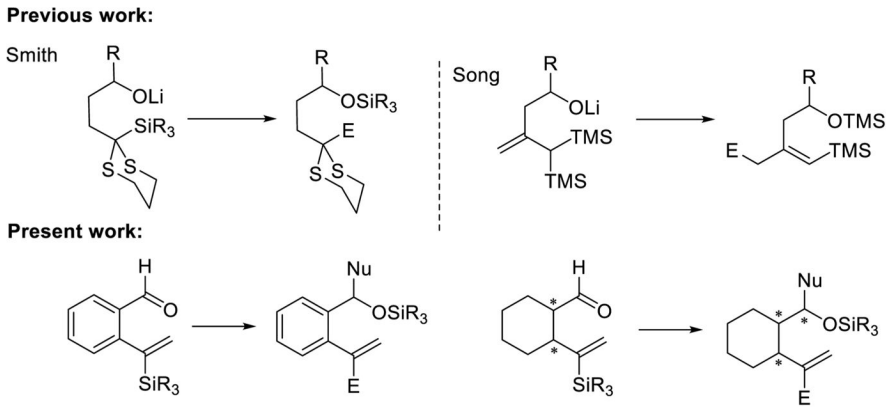

Figure 1.
Previous and present work: union reaction exploiting [1,5]-Brook rearrangements.

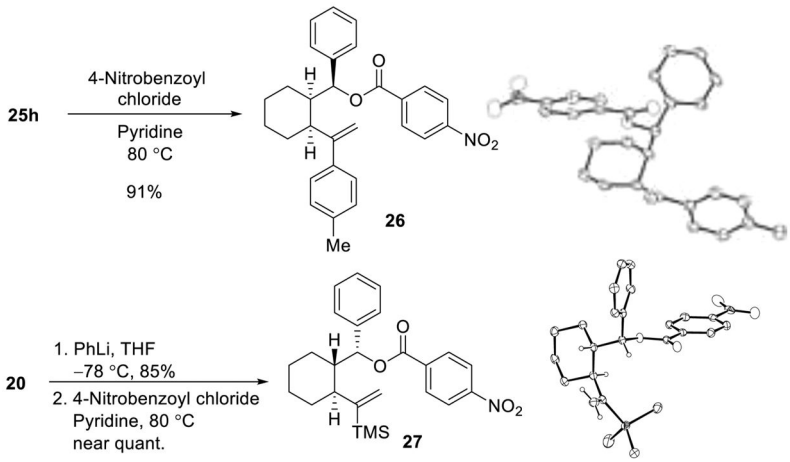

Figure 2.
Elucidation of relative configuration via X-ray analysis.

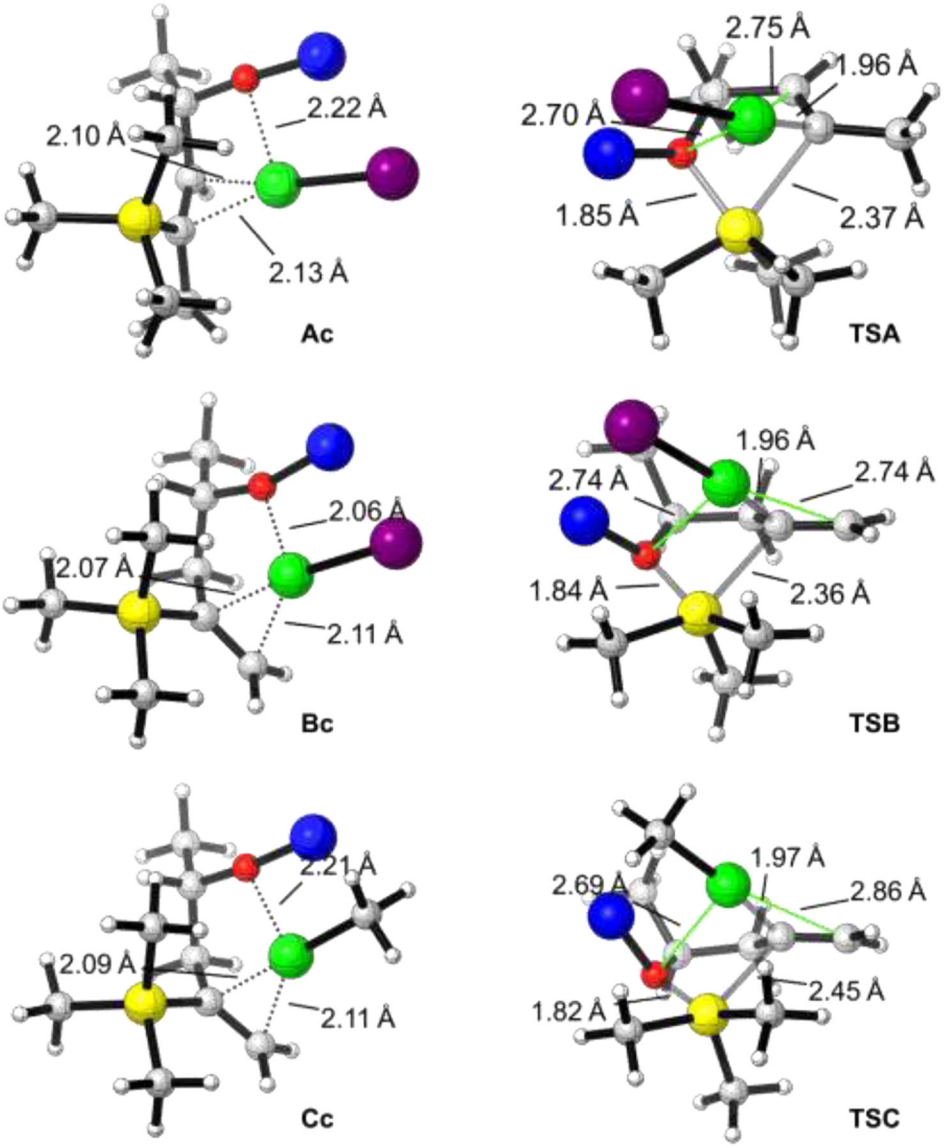

Figure 3.

DFT-optimized structures of intermediates and transition states for [1,4]-vinyl Brook rearrangements; carbon gray, hydrogen white, oxygen red, silicone yellow, lithium blue, copper green, and iodine purple.

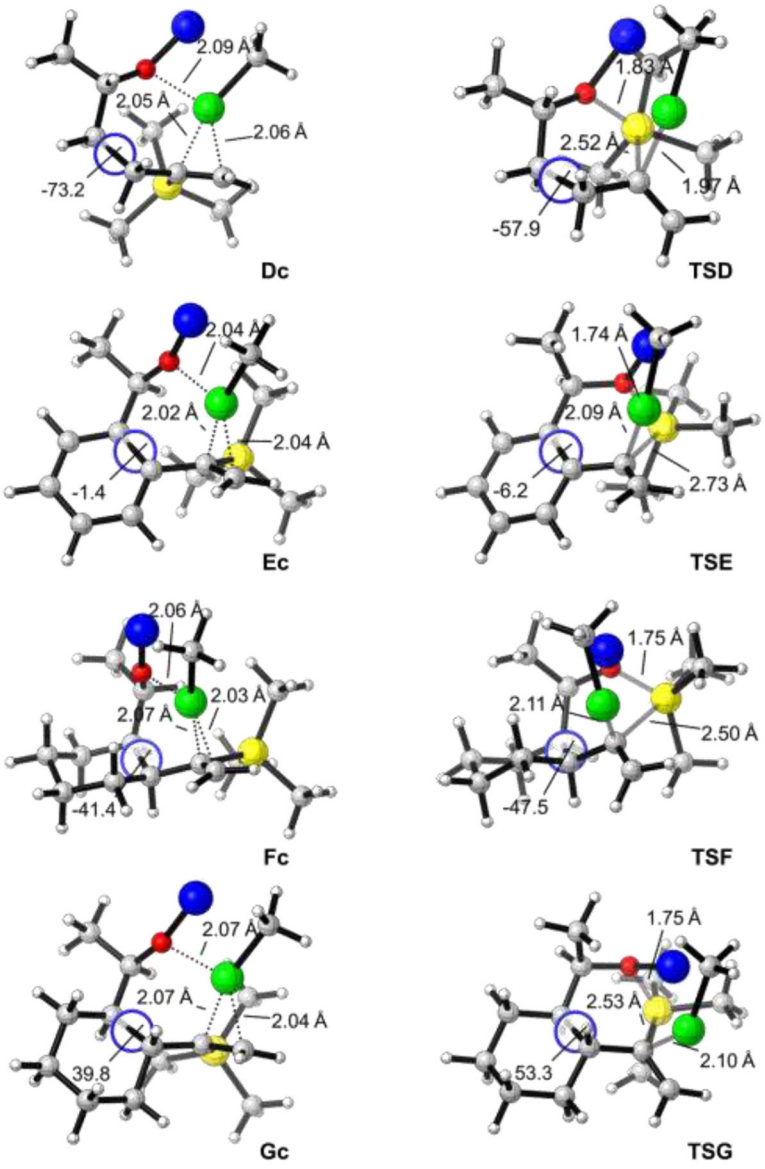

Figure 4.

DFT-optimized structures of intermediates and transition states for [1,5]-vinyl Brook rearrangements; carbon gray, hydrogen white, oxygen red, silicone yellow, lithium blue, and copper green.

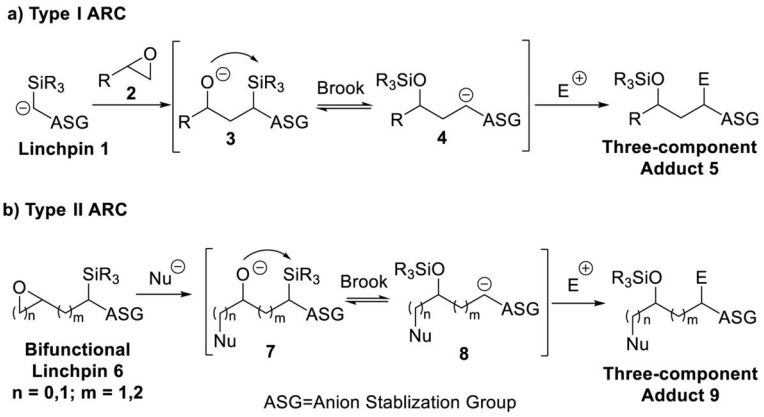

Scheme 1.

Anion Relay Chemistry: Type I and Type II

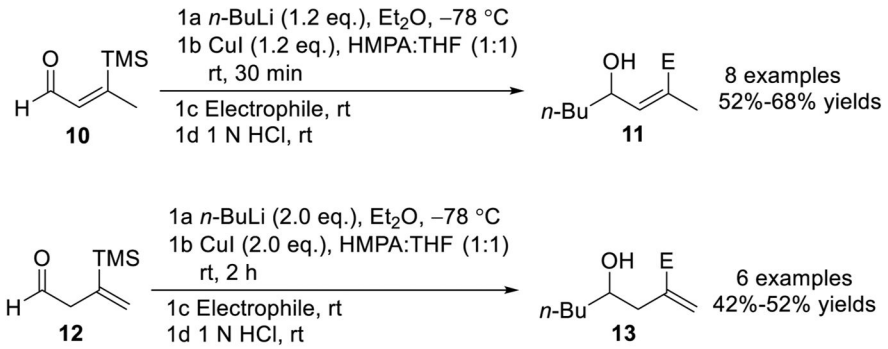

Scheme 2.
Type II ARC with [1,4]-Brook Rearrangement

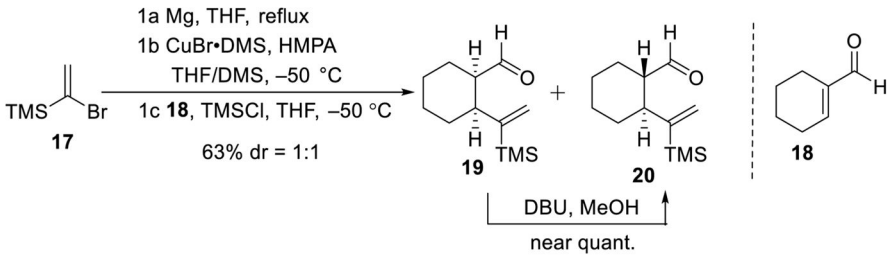

Scheme 3.
Preparation of Cyclohexyl Incorporated Linchpins 19 and 20

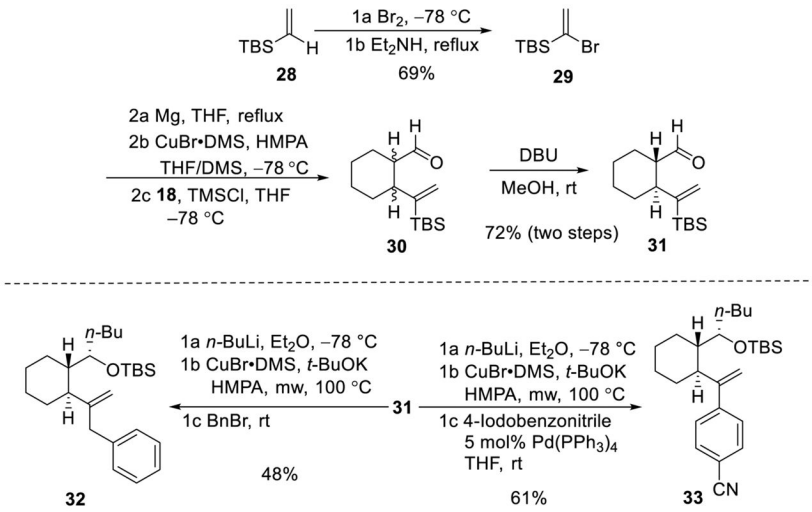

Scheme 4.

Synthesis and Evaluation of *trans* Linchpin 31

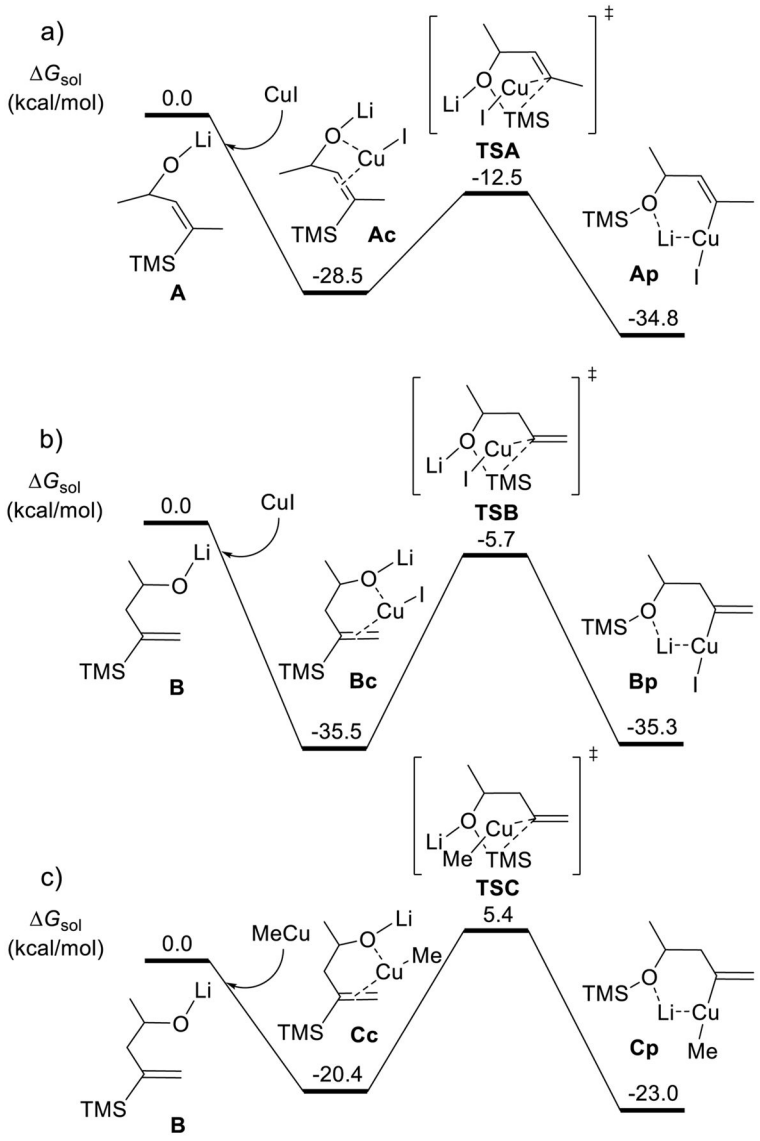

Scheme 5.

Comparisons of [1,4]-Vinyl Brook Rearrangements Involving Different Substrates and Copper Reagents

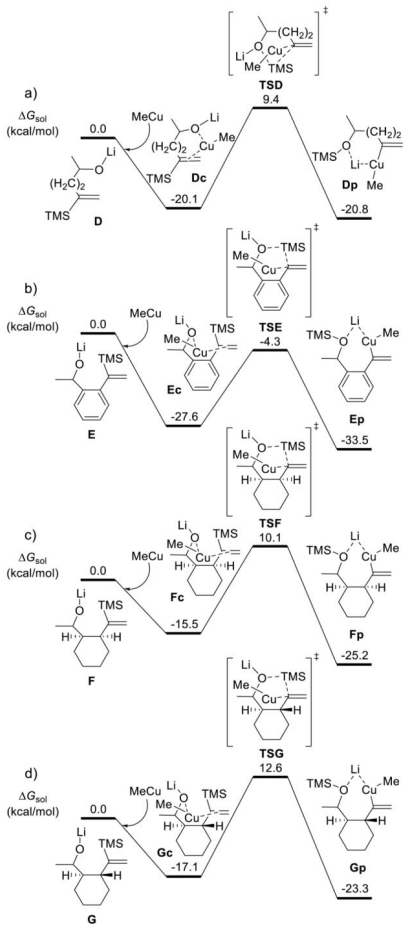

Scheme 6.

Comparisons of [1,5]-Vinyl Brook Rearrangements Involving Dierent Substrates

Table 1

Three-Component Coupling of Linchpin 14 via ARC/Alkylation

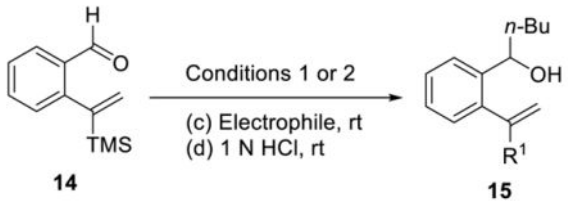

14 **15**

electrophile	R^1	yield
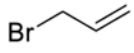	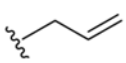	73%[a] (74%)[b]
	15a	
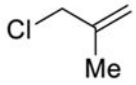	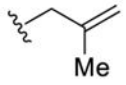	68%[a] (73%)[b]
	15b	
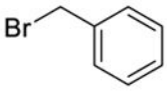	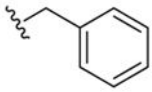	70%[a] (73%)[b]
	15c	
Mel		(77%)[b]
	15d	
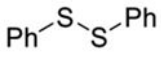	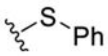	61%[a] (56%)[b]
	15e	

[a]Conditions 1: (a) 2.0 equiv of *n*-BuLi, Et_2O, −78 °C; (b) 2.0 equiv of CuBr·DMS, HMPA/THF (1:1), rt; then (c) and (d).

[b]Conditions 2: (a) 1.1 equiv of *n*-BuLi, THF, −78 °C; (b) 2.0 equiv of CuBr·DMS, 1.0 equiv of *t*-BuOK, HMPA, rt; then (c) and (d).

Table 2

Three-Component Coupling of Linchpin 14 via ARC/CCR

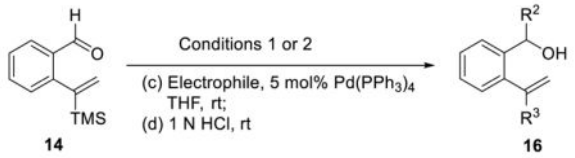

nucleophile	electrophile	R^2	R^3	yield
n-BuLi	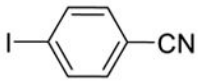	*n*-Bu	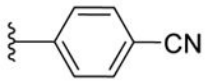	72%[a] (70%)[b]
			16a	
n-BuLi	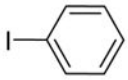	*n*-Bu	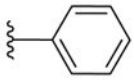	77%[a] (71%)[b]
			16b	
n-BuLi	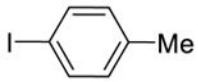	*n*-Bu	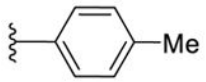	73%[a] (78%)[b]
			16c	
n-BuLi	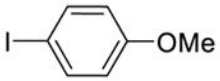	*n*-Bu	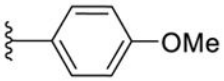	72%[a] (76%)[b]
			16d	
n-BuLi		*n*-Bu		75%[a] (78%)[b]
			16e	
MeLi	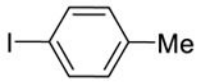	Me	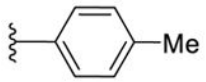	70%[a] (69%)[b]
			16f	
PhLi	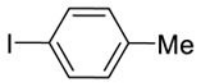	Ph	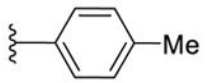	63%[a] (57%)[b]
			16g	
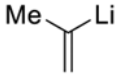	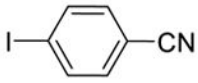	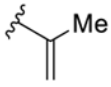	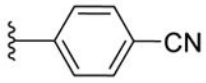	(69%)[b]
			16h	

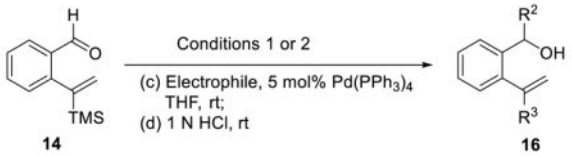

nucleophile	electrophile	R^2	R^3	yield
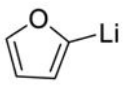	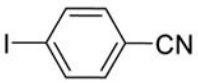	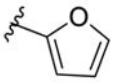	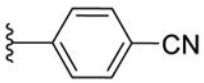	(57%)[b,c]
			16i	
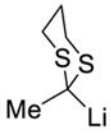	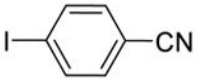	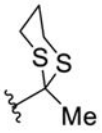	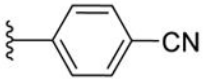	(53%)[b,d]
			16j	

[a] Conditions 1: (a) 2.0 equiv of nucleophile, Et_2O, −78 °C; (b) 2.0 equiv of CuBr·DMS, HMPA/THF (1:1), rt; then (c) and (d).

[b] Conditions 2: (a) 1.1 equiv of nucleophile, THF, −78 °C; (b) 2.0 equiv of CuBr·DMS, 1.0 equiv of *t*-BuOK, HMPA, rt; then (c) and (d).

[c] For conditions 2, step b, 60 °C.

[d] for conditions 2, step a, rt.

Table 3

Optimization of [1,5]-Brook Rearrangement with *cis* Linchpin 19

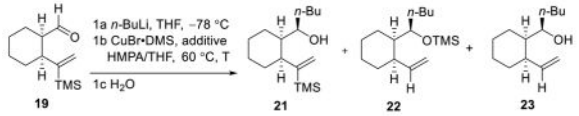

entry	*n*-BuLi (equiv)	Cu(I) (equiv)	additive (equiv)	HMPA/THE	*T* (h)	ratio[a] (21/22/23)
1[b]	1.1			1:1	0.5	1:0: 0
2	1.1	1.2		1:1	6	1:0: 0
3	1.1	2.0		1:1	6	1:0.2:0.1
4	1.5	2.0		1:1	3	0.1:1: 0.7
5	2.0	2.0		1:1	0.75	0:1: 0
6	1.1	2.0	1.0[c]	1:1	1.5	0.1:1: 0.7
7[d]	1.1	2.0	1.0[c]	1:0	0.75	0:1: 0

[a]Ratio of major products (**21**/**22**/**23**) by NMR analysis of the reaction mixture: values are reported as 0 if less than 0.05.

[b]Isolated yield for product **21**: 86%.

[c]*t*-BuOK.

[d]Isolated yield for product **22**: 73%.

Table 4

Three-Component Coupling of Linchpin 19 via ARC/Alkylation

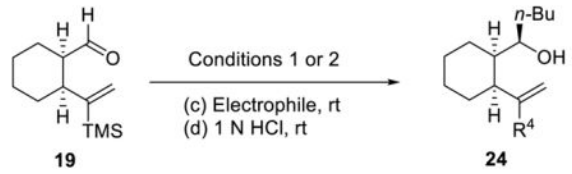

electrophile	R^4	yield
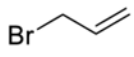	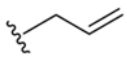 **24a**	63%[a] (63%)[b]
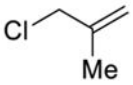	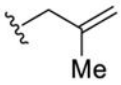 **24b**	54%[a] (67%)[b]
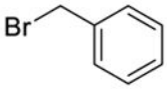	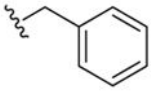 **24c**	66%[a] (71%)[b]
Mel	 **24d**	(65%)[b]
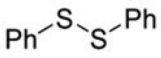	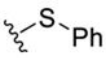 **24e**	45%[a] (53%)[b]

[a]Conditions 1: (a) 2.0 equiv of *n*-BuLi, THF, −78 °C; (b) 2.0 equiv of CuBr·DMS, HMPA/THF (1:1), 60 °C; then (c) and (d).

[b]Conditions 2: (a) 1.1 equiv of *n*-BuLi, THF, −78 °C; (b) 2.0 equiv of CuBr·DMS, 1.0 equiv of *t*-BuOK, HMPA, 60 °C; then (c) and (d).

Table 5

Three-Component Coupling of Linchpin 19 via ARC/CCR

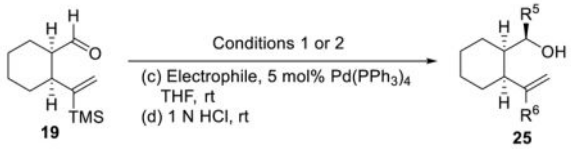

nucleophile	electrophile	R^5	R^6	yield
n-BuLi	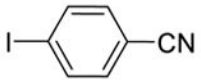	*n*-Bu	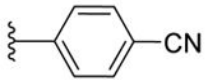 **25a**	49%[a] (53%)[b]
n-BuLi	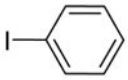	*n*-Bu	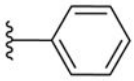 **25b**	61%[a] (57%)[b]
n-BuLi	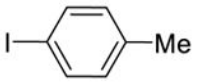	*n*-Bu	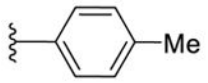 **25c**	54%[a] (59%)[b]
n-BuLi	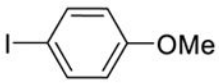	*n*-Bu	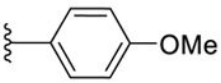 **25d**	55%[a] (62%)[b]
n-BuLi	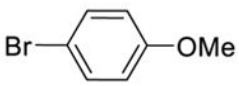	*n*-Bu	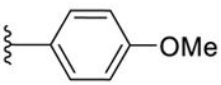 **25e**	(55%)[b]
n-BuLi		*n*-Bu	 **25f**	(68%)[b]
MeLi	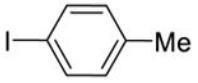	Me	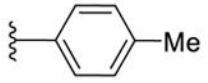 **25g**	55%[a] (51%)[b]
PhLi	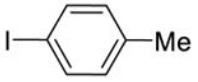	Ph	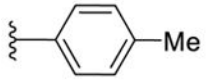 **25h**	63%[a] (52%)[b]

[a] Conditions 1: (a) 2.0 equiv of nucleophile, THF, −78 °C; (b) 2.0 equiv of CuBr·DMS, HMPA/THF (1:1), 60 °C; then (c) and (d).

[b] Conditions 2: (a) 1.1 equiv of nucleophile, THF, −78 °C; (b) 2.0 equiv of CuBr·DMS, 1.0 equiv of *t*-BuOK, HMPA, 60 °C; then (c) and (d).